Local dielectric permittivity of HfO_2 based slabs and stacks: A first principles study

N. Shi[a] and R. Ramprasad
Department of Chemical, Materials and Biomolecular Engineering, Institute of Materials Science, University of Connecticut, 97 N. Eagleville Road, Storrs, Connecticut 06269, USA

(Received 31 July 2007; accepted 19 November 2007; published online 14 December 2007)

A recently developed theory of atomic-scale local dielectric permittivity has been used to determine the position dependent optical and static dielectric permittivity profiles of a few nanoscale HfO_2 and $Si-HfO_2$ heterojunction slabs. The dielectric constants at the interior regions of each component recovered their respective bulk values. Enhancement of the dielectric constant at the free surfaces and its variations at the $Si-HfO_2$ interface could be correlated to the corresponding surface and interfacial chemistry. © *2007 American Institute of Physics*. [DOI: 10.1063/1.2822834]

Owing to its high dielectric constant, high thermal stability, and large band offsets with respect to silicon, hafnia (HfO_2) has emerged as the most promising candidate for the replacement of currently used SiO_2 gate dielectrics in metal-oxide-semiconductor transistors.[1,2] However, the $Si-HfO_2$ interface is poorly understood due to its complicated interfacial structure, especially as interfacial phases not allowed by bulk thermodynamics tend to form.[3–6]

Moreover, as insulator thickness in multilayered systems shrink to the nanoscale, the structure and chemistry at interfaces could significantly influence their dielectric response. Our recent work on the scaling with thickness of the dipole moment induced due to an external electric field in ultrathin SiO_2 (Ref. 7) and HfO_2 (Ref. 8) slabs indicates that the dielectric properties in the surface regions are considerably different from those of the bulk. Nevertheless, a quantitative estimation of the dielectric constant or polarization at surface and interface regions was not possible using this approach. More recently, using the theory of the local dielectric permittivity,[9–11] position-dependent polarization and dielectric constant profiles across single-component Si and SiO_2 slabs, and two-component $Si-SiO_2$ multilayers were determined.[9–11] These computations allowed for a correlation of the local surface and interfacial chemistry on the one hand, and their dielectric response on the other.

In this paper, using the theory of the local permittivity and first principles computations based on density functional theory (DFT),[12] we determine static and optical dielectric constant profiles across HfO_2 slabs and coherent $Si-HfO_2$ interfaces. Although idealized situations such as coherent interfaces are considered here, this approach can be extended to more realistic situations involving disorder, defects, or nonequilibrium phases at the $Si-HfO_2$ interfaces.

All calculations were performed using the local density approximation within DFT (Ref. 12) as implemented in the local orbital SIESTA code.[13] Norm-conserving nonlocal pseudopotentials of the Troullier-Martins type were used to describe all the elements. The atomic configuration $[\text{Kr}\ 4d^{10}4f^{14}5s^25p^6]5d^26s^2$ was used for the Hf pseudopotential, $[\text{He}]2s^22p^4$ for the O pseudopotential, and $[\text{Ne}]3s^23p^2$ for Si pseudopotential. Semicore corrections were used for Hf and Si. A double-zeta plus polarization basis set was used for all calculations. An energyshift parameter of 0.0001 Ry was used to result in well converged polarization and dielectric constant profiles. The number of special **k** points that yielded well converged bulk and slab results for HfO_2 in the cubic phase were 108 and 36, those for HfO_2 in the tetragonal phase were 74 and 28, and for the $Si-HfO_2$ heterjunction was 18, respectively. A set of 75 special **k** points were used to treat bulk Si. The equilibrium positions of all atoms were determined by requiring the forces on each atom to be smaller than 0.01 eV/Å.

With the above stringent choice of parameters, a value of 5.43 Å was obtained for the equilibrium lattice constant of bulk Si in the diamond crystal structure, identify to the experimental value.[14] The equilibrium lattice constant of cubic HfO_2 was calculated to be 5.02 Å, and the a and c equilibrium lattice constants of tetragonal HfO_2 were calculated to be 4.99 and 5.06 Å, respectively. These results are in good agreement with the prior DFT results[15,16] of 5.04 Å for cubic HfO_2, and 5.03 and 5.11 Å for tetragonal HfO_2. The corresponding experimental lattice constants[17,18] are 5.08 Å for cubic HfO_2, and 5.15 and 5.29 Å for the tetragonal case.

The position-dependent optical and static dielectric constant profiles for HfO_2 and $Si-HfO_2$ heterojunction slabs were computed as briefly described below (and in detail elsewhere[9,10]). The geometry of the slabs in the absence of an external electric field was optimized first. An electric field of strength $\pm\delta$ (with $\delta=0.01$ V/Å) was then applied along the direction normal to the surface or interface (say, the z direction), and the field induced total charge density was calculated as the difference between the total charge density due to fields of $+\delta$ and $-\delta$. Our choice of the value of δ ensures that both Si and HfO_2 are in the linear regime. In fact, prior work has indicated that Si, SiO_2, and HfO_2 are linear at fields as high as 0.1 V/Å.[7–9]

The local position-dependent polarization induced due to an external field along the z direction is given by[19]

$$\frac{d}{dz}\bar{p}(z) = -\bar{\rho}_{\text{ind}}(z), \tag{1}$$

where the $\bar{p}(z)$ and $\bar{\rho}_{\text{ind}}(z)$ are the polarization and field-induced charge density along the z axis, respectively, averaged on the x-y plane. The solution of Eq. (1) with the appropriate boundary condition (zero polarization in the middle of the vacuum regions of the supercell) provides the planar

[a]Electronic mail: nis02002@engr.uconn.edu

© 2007 American Institute of Physics
Downloaded 14 Dec 2007 to 137.99.26.43. Redistribution subject to AIP license or copyright; see http://apl.aip.org/apl/copyright.jsp

averaged position-dependent polarization, from which the position-dependent local dielectric constant profile (for linear systems, such as the ones considered here) can be determined as

$$\epsilon(z) = \frac{\epsilon_0 E_{\text{ext}}}{\epsilon_0 E_{\text{ext}} - \bar{p}(z)}, \tag{2}$$

In the present work, $E_{\text{ext}}=2\delta=0.02$ V/Å, as $\bar{p}(z)$ was determined from charge densities due to fields of $+\delta$ and $-\delta$ along the z direction separately. Our choice of $\pm\delta$ for the electric fields, rather than 0 and $+\delta$ (or $-\delta$), was entirely due to numerical reasons. For the same level of convergence of the charge density, our choice of symmetric electric fields results in a more accurate polarization profile with reduced numerical noise due to a more complete cancelation of errors. The optical (or high frequency) part of the polarization and dielectric constant was obtained by fixing the atomic positions at their field-free equilibrium values, and the total static (or low frequency) behavior was determined by allowing the atoms to relax to their field-induced equilibrium positions.[9,10]

Hf-terminated (001) cubic and tetragonal HfO_2 slabs were considered, with thickness along the z direction of 18.40 and 18.63 Å, respectively. These slabs containing nine layers of Hf were found to be sufficiently thick to ensure a bulklike region in the interior of the slabs, as evidenced by negligible surface relaxations in the interior. The calculated static and optical dielectric constant $\epsilon(z)$ profiles for the cubic and tetragonal HfO_2 slabs are shown in Fig. 1. It can be seen that both the static and optical dielectric constants at the interior region of the slabs approach their corresponding bulk values. For the cubic phase, the static and optical dielectric constants extracted from the interior of HfO_2 slabs were 5.3 and 30.4, respectively, and those for the tetragonal phase were 5.2 and 16.7, respectively, in good agreement with our prior work,[8] other DFT determinations,[16] and experiments.[20,21] For instance, we have estimated the optical and static parts of the dielectric constant of bulk cubic HfO_2 to be 5 and 29, respectively,[8] and Zhao and Vanderbilt[16] have obtained corresponding values of 5 and 29 for the cubic phase, and 5 and 15.7 for the tetragonal phase along the c axis. At the surface regions, we find that there is an enhancement of the dielectric constants, compared to that of the bulk values. The deviation at the surface stems from the undercoordination of surface Hf atoms; Mulliken charge analysis indicated that surface Hf atoms are closer to a +2 charge states, as opposed to Hf atoms in the interior of the slabs which were closer to a +4 charge state. The coordinative unsaturations render the surface atoms more polarizable, similar to previous results for SiO_2 surfaces.[9] The more pronounced oscillatory behavior of the static dielectric constant displayed at the surface of the cubic phase is consistent with its larger field-induced surface relaxations (and the sensitivity of the dielectric response to even slight changes in atomic positions). The field-induced changes in the surface relaxation of the three outermost Hf layers, Δd_{12} and Δd_{23}, were 0.05% and 0.02%, respectively, in the cubic phase, while these values were 0.01% and 0.01%, respectively, in the tetragonal phase.

The dielectric constant profile of the (001) silicon slab has been reported in our previous study.[9,10] We found that the optical and static dielectric constant attain constant values of about 12 in the interior of the slabs, in good agreement with the experimental bulk Si value of 12.1.[22] Enhancement of the dielectric constant at surface regions is again due to the underpassivation of the surface atoms.

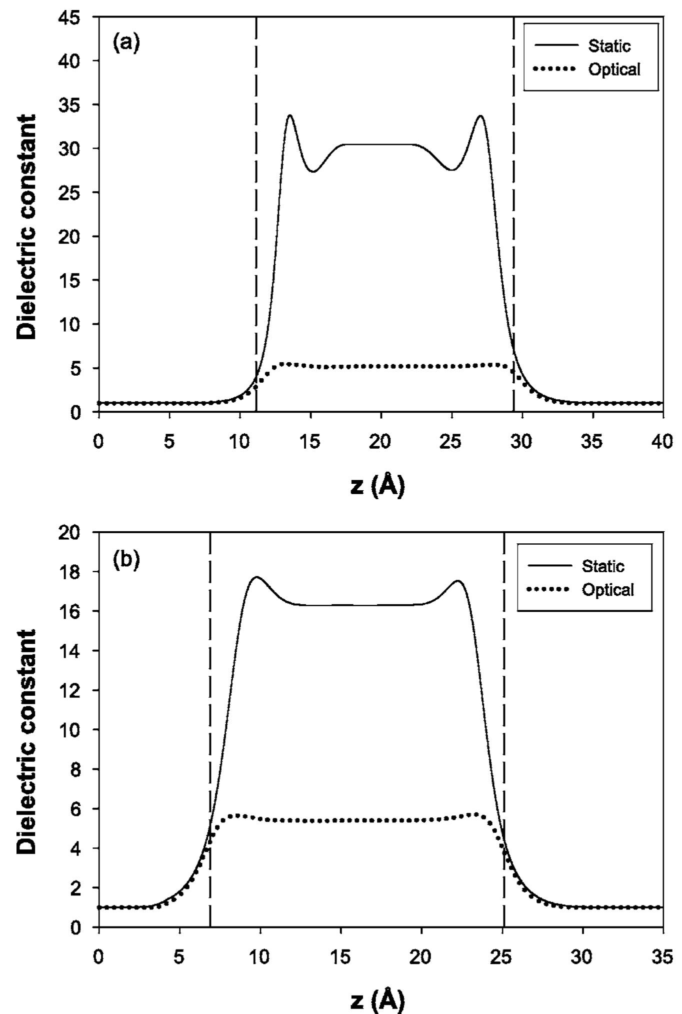

FIG. 1. Static (solid) and optical (dotted) planar-averaged dielectric constants of (001) HfO_2 slabs in the cubic (a) and tetragonal (b) phases as a function of z position normal to the surface. Vertical dashed lines indicate positions of the free surfaces.

An expitaxial $Si-HfO_2$ interface model[23] was created by placing a (001) cubic HfO_2 slab on Si such that the HfO_2 slab was coherently matched on top of Si at its equilibrium lattice constant. The interface model contained up to 9 Si, 8 Hf, and 18 O layers, with the thickness of Si and HfO_2 layers being 12.20 and 18.20 Å, respectively. In the resulting relaxed structure, half the interface O atoms move toward Si, and the other half move toward the Hf layer, as shown in the top part of Fig. 2. Thus, Si–O–Si and Hf–O–Hf bonds are formed at the interface, thereby passivating all interfacial Si and Hf atoms, consistent with the bond-counting rules proposed earlier for this system.[4] This "rumpling" of the O layers persists into the HfO_2 part of the heterostructure, resulting in a structure equivalent to tetragonal HfO_2.

The position-dependent dielectric constant normal to the $Si-HfO_2$ interface determined using the procedure described above is shown in Fig. 2. It can be seen that the dielectric constants in the interior of the HfO_2 and Si regions again match well with the corresponding experimental bulk values (the static and optical permittivities of the interior part of HfO_2 are in fact almost identical to those of tetragonal

Downloaded 14 Dec 2007 to 137.99.26.43. Redistribution subject to AIP license or copyright; see http://apl.aip.org/apl/copyright.jsp

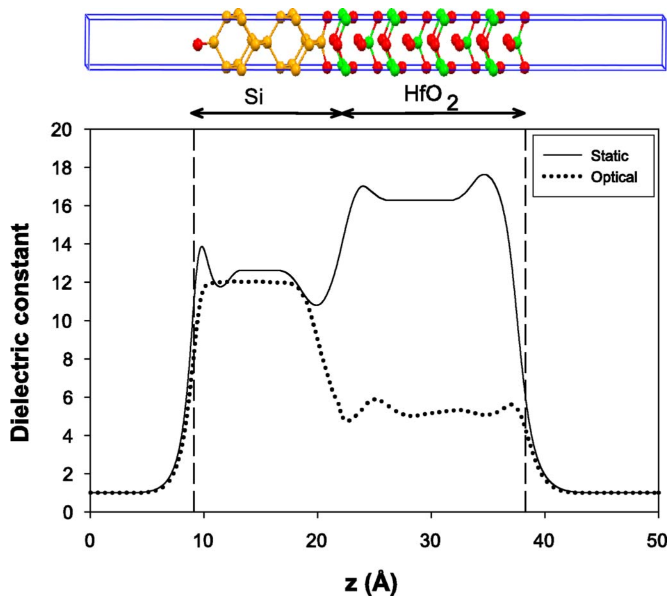

FIG. 2. (Color online) Above: atomic model of Si–HfO_2 interface with O termination, with Si atom shown in gold, O in red, and Hf in green. The supercell repeats in the *x*-*y* dimensions and has finite thickness along the *z* direction normal to the interface. Below: static (solid) and optical (dotted) planar-averaged dielectric constants of (001) Si–HfO_2 interface as a function of *z* position normal to the interface.

HfO_2). The enhancement of the permittivities at the free surfaces compared to the corresponding bulk values can be seen here as well, again due to the underpassivation of surface atoms. The Si–HfO_2 interface displays interesting behavior. The static dielectric constant enhancement at the HfO_2 side of the interface is lower than that at the HfO_2 free surface, due to the passivation provided by the formation of the Hf–O–Hf bonds at the Si–HfO_2 interface. The pronounced decrease of the static dielectric constant at the Si side of the interface is due to the formation Si–O–Si bonds similar to that in the suboxide region at Si–SiO_2 interfaces observed earlier to have a moderate dielectric constant of about 7.[24] Indeed, Mulliken charge analysis indicates that interfacial Hf atoms are in oxidation states closer to that in bulk HfO_2 than in Hf atoms at the free surface, and interfacial Si atoms are in an oxidation state of about +2, intermediate between that of Si in bulk Si (0) and in SiO_2 (+4). The dielectric response is thus intimately tied to the local chemistry, reminiscent of the behavior displayed by Si–SiO_2 interfaces.[9–11] (We do note that, interestingly, the optical part of the dielectric constant displays less pronounced variations at surfaces and interfaces, and are thus less sensitive to local chemistry.) Such sensitive structure-property correlations pertaining to the static dielectric constant could have important implications for the dielectric properties of real Si–HfO_2 interfaces. Owing to the idealized nature of the systems considered here, we do not observe dramatic changes in the interfacial dielectric response. Nevertheless, given the tendency for the formation of nonequilibrium phases[3–6] at realistic Si–HfO_2 interfaces, e.g., through interfacial segregation of point defects,[23,25] such sensitive correlations between the interfacial chemistry and dielectric response could have adverse implications for devices containing high-*k* materials. The current work constitutes an initial effort toward understanding such realistic interfaces.

In summary, atomic-scale dielectric constant profiles for ultrathin HfO_2 slabs and a coherent Si–HfO_2 heterojunction have been determined using the theory of the local dielectric permittivity and DFT computations. The bulk static and optical dielectric constant values of each component were recovered within a few atomic bond distances from surfaces and interfaces. The deviation of the dielectric constant values at surfaces and interfaces from the corresponding bulk values could be correlated to the local bonding and chemistry.

Support of this work by grants from the ACS Petroleum Research Fund, the National Science Foundation, and the Office of Naval Research is gratefully acknowledged.

[1]G. D. Wilk and D. A. Muller, Crit. Rev. Solid State Mater. Sci. **28**, 231 (2003).
[2]J. Roberson, Rep. Prog. Phys. **69**, 327 (2006).
[3]V. Fiorentini and G. Gulleri, Phys. Rev. Lett. **89**, 266101 (2002).
[4]P. W. Peacock, K. Xiong, K. Y. Tse, and J. Robertson, Phys. Rev. B **73**, 075328 (2006).
[5]E. Cockayne, Phys. Rev. B **75**, 094103 (2007).
[6]R. K. Nahar, V. Singh, A. Sharma, J. Mater. Sci.: Mater. Electron. **18**, 615 (2007).
[7]N. Shi and R. Ramprasad, Appl. Phys. Lett. **87**, 262102 (2005).
[8]R. Ramprasad and N. Shi, Phys. Rev. B **72**, 052107 (2005).
[9]N. Shi and R. Ramprasad, Phys. Rev. B **74**, 045318 (2006).
[10]N. Shi and R. Ramprasad, J. Comput.-Aided Mater. Des. **10820**, 133 (2006).
[11]F. Giustino and A. Pasquarello, Phys. Rev. B **71**, 144104 (2005).
[12]R. Martin, *Electronic Structure: Basic Theory and Practical Methods* (Cambridge University Press, New York, 2004).
[13]J. M. Soler, E. Artacho, J. Gale, A. Garcia, J. Junquera, P. Ordejon, and D. Sanchez-Portal, J. Phys.: Condens. Matter **14**, 2745 (2002).
[14]Data collected by C. Kittel, *Introdunction to Solid State Physics*, 5th ed. (Wiley, New York, 1976), and references therein.
[15]A. A. Demkov, Phys. Status Solidi B **226**, 57 (2001).
[16]X. Zhao and D. Vanderbilt, Phys. Rev. B **65**, 233106 (2002).
[17]J. Wang, H. Li, and R. Stevens, J. Mater. Sci. **27**, 5397 (1992).
[18]J. Adam and M. D. Rodgers, Acta Crystallogr. **12**, 951 (1959).
[19]J. D. Jackson, *Classical Electrodynamics* (University of California, Berkeley, 1998).
[20]X. Zhao and D. Vanderbilt, Phys. Rev. B **65**, 075105 (2002).
[21]G.-M. Rignanese, X. Gonze, G. Jun, K. Cho, and A. Pasquarello, Phys. Rev. B **69**, 184301 (2004).
[22]C. A. Balans, *Advanced Engineering Electromagnetics* (Arizona State University, New York, 1989).
[23]C. Tang, B. Tuttle, and R. Ramprasad, Phys. Rev. B **76**, 073306 (2007).
[24]C. M. Perkins, B. B. Triplett, P. C. McIntyre, K. C. Saraswat, S. Haukka, and M. Touminen, Appl. Phys. Lett. **78**, 2357 (2001).
[25]C. Tang and R. Ramprasad, Phys. Rev. B **75**, 241302 (2007).

Downloaded 14 Dec 2007 to 137.99.26.43. Redistribution subject to AIP license or copyright; see http://apl.aip.org/apl/copyright.jsp